Acta Oceanologica Sinica 2006, Vol. 25, No. 1, p. 1~14
http://www.oceanpress.com.cn
E-mail: hyxbe@263.net

Observation of ocean current response to 1998 Hurricane Georges in the Gulf of Mexico

ZHENG Quanan[1*], LAI Ronald J[2], HUANG Norden E[3], PAN Jiayi[4], LIU W Timothy[5]

1. Department of Atmospheric and Oceanic Science, University of Maryland, College Park, Maryland 20742, USA
2. Minerals Management Service, U S Department of the Interior, Herndon, Virginia 20170, USA
3. Ocean and Ice Branch, NASA Goddard Space Flight Center, Greenbelt, Maryland 20771, USA
4. Department of Environmental and Biomolecular Systems, Oregon Graduate Institute, Beaverton, Oregon 97006, USA
5. Jet Propulsion Laboratory, California Institute of Technology, Pasadena, California 91109, USA

Received 17 September 2005; accepted 9 December 2005

Abstract

The ocean current response to a hurricane on the shelf-break is examined. The study area is the DeSoto Canyon in the northeast Gulf of Mexico, and the event is the passage of 1998 Hurricane Georges with a maximum wind speed of 49 m/s. The data sets used for analysis consist of the mooring data taken by the Field Program of the DeSoto Canyon Eddy Intrusion Study, and simultaneous winds observed by NOAA (National Oceanic and Atmospheric Administration) Moored Buoy 42040. Time-depth ocean current energy density images derived from the observed data show that the ocean currents respond almost immediately to the hurricane with important differences on and off the shelf. On the shelf, in the shallow water of 100 m, the disturbance penetrates rapidly downward to the bottom and forms two energy peaks, the major peak is located in the mixed layer and the secondary one in the lower layer. The response dissipates quickly after external forcing disappears. Off the shelf, in the deep water, the major disturbance energy seems to be trapped in the mixed layer with a trailing oscillation; although the disturbance signals may still be observed at the depths of 500 and 1 290 m. Vertical dispersion analysis reveals that the near-initial wave packet generated off the shelf consists of two modes. One is a barotropic wave mode characterized by a fast decay rate of velocity amplitude of 0.020 s^{-1}, and the other is baroclinic wave mode characterized by a slow decay rate of 0.006 9 s^{-1}. The band-pass-filtering and empirical function techniques are employed to the frequency analysis. The results indicate that all frequencies shift above the local inertial frequency. On the shelf, the average frequency is 1.04f in the mixed layer, close to the diagnosed frequency of the first baroclinic mode, and the average frequency increases to 1.07f in the thermocline. Off the shelf, all frequencies are a little smaller than the diagnosed frequency of the first mode. The average frequency decreases from 1.035f in the mixed layer to 1.02f in the thermocline, implying a trend for the shift in frequency of the oscillations towards f with the depth.

Key words: shelf dynamics, hurricane, ocean current, air-sea interaction

1 Introduction

Hurricane is an extremely high wind event, which injects momentum into the oceanic mixed layer along its passage for a very short duration. If our interest is not at the surface, but in a depth away from the immediate surface wave influence, then the generation of near-inertial oscillations becomes an important feature of the ocean response to the winds. In fact, wind-driven near-inertial motion has constituted a critical area of investigation in recent years. These near-inertial oscillations are characterized by frequencies near the local inertial frequency $f(=2\Omega \sin\theta$, the Coriolis parame-

* Corresponding author, E-mail: quanan@atmos.umd.edu

ter). Numerous field observations show that the fluctuation of the peak-to-peak amplitude of the ocean current induced by the near-inertial oscillations may reach an order of 100 cm/s, implying that they are significant components for upper ocean dynamics. Using a suddenly rising constant wind stress to drive a geostrophically balanced ocean, Gold (1908) obtained a wave solution, which oscillates with the inertial frequency and the amplitude depending on the wind stress. Many investigators have used this theoretical model to explain observations (Pollard, 1970; Halpern, 1974; Kundu, 1976). Chang and Anthes (1978) investigated the ocean response to moving hurricanes with numerical simulations. Price (1981) investigated the ocean response to a moving hurricane with emphasis on sea surface temperature response. Greatbatch (1983, 1984) used the nonlinear equations and numerical method to study the ocean response to a moving storm. Gill (1984) proposed a normal mode method used for analyzing the behavior of baroclinic near-inertial waves in the wakes of storms. Chang (1985) examined the ocean response to 1975 Hurricane Eloise and indicated that the ocean response consists of two components: barotropic response and baroclinic response. Shay and Elsberry (1987) and Shay et al. (1992) observed the ocean response to the passages of hurricanes in the Gulf of Mexico.

The purpose of this study is to examine the ocean current response to a hurricane on the shelf-break using continuous wind and ocean current time series. The ocean current data sets have a season-long coverage, 30 minute temporal resolution, and 6 m depth resolution in the mixed layer and the thermocline. We will focus attention on the behavior of pre-existing near-inertial oscillations when they are forced by a hurricane.

2 Study area and field program

Our study area, the Gulf of Mexico, is located at the pathway of tropical storms and hurricanes (Shay and Elsberry, 1987; Shay et al., 1992; Keen and Allen, 2000). During summer and fall of 1998, two hurricanes (Earl and Georges) passed through the region and three tropical storms (Charley, Frances, and Hermine) were formed in the region. Our study area is the DeSoto Canyon centered at 29° N, 87.5° W in the northeast Gulf of Mexico as shown in Fig.1. The canyon is an important geological feature which is a channel for exchange of nearshore and offshore flows. The data used for this study are taken by the Field Pro-

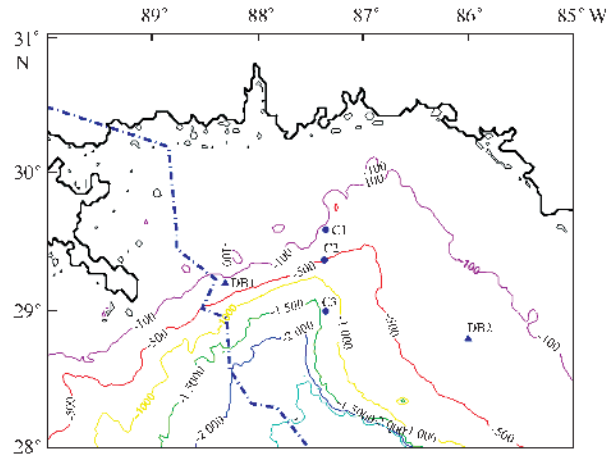

Fig. 1. A map of the study area. DB1 and DB2 represent the locations of NOAA Moored Buoys 42040 and 42039. Stations C1, C2, and C3 are mooring stations of the Field Program of the DeSoto Canyon Intrusion Study. The dash-dot line represents the track of 1998 Hurricane Georges plotted with NOAA data.

gram of the DeSoto Canyon Eddy Intrusion Study from 1996 to 1999. Fourteen moorings along three isobaths were deployed to investigate the local circulation and physical processes, which may have effects on flow patterns and exchange mechanisms. Three years of data were collected within a region with the water depth ranging from 100 to 1 300 m (Minerals Management Service, 1999). Beside mooring data, other hydrographic data, meteorological data, and satellite images were also collected. We have chosen two mooring stations C1 and C3 marked in Fig. 1, to examine the ocean current response to the hurricane on the shelf-break. Station C1 is located at 29°35.210′N, 87°20.972′W.

The water depth is 100 m, and the instrument-measured depth is 95 m. The offshore distance is 80 km. Station C1 is chosen to represent the shallow water side of the shelf-break. Station C3 is located at 29°00.191′N, 87°21.387′W. The water depth is 1 300 m, and the maximum instrument-measured depth is 1 290 m. The offshore distance is 150 km. Station C3 is chosen to represent the deep water side of the shelf-break. The two stations do not have wind sensors. Instead, the winds measured by the nearest NOAA Moored Buoy 42040 are used to calculate the wind stress of the hurricane. The buoy is located at 29°12′36″N, 88°12′00″W, as marked by DB1 in Fig. 1. The buoy is located near the path of 1998 Hurricane Georges center. The details of these mooring stations are listed in Table 1.

Table 1. Mooring stations used for this study

Station center	Location	Water depth/m	Instrument depth/m	Instrument type	Distance to hurricane/km
C1	29°35.210'N	100	20	CTD	114($2.9R_{max}$)
	87°20.972'W		80	ADCP	
			82	CT	
			95	RCM-7	
C3	29°00.919'N	1 300	80	ADCP	93($1.7R_{max}$)
	87°21.198'W		500	MK2	
			1 290	RCM-8	
NOAA Buoy 42040	29°12'36"N 88°12'00"W	238	5(height)	anemometer	5

3 Hurricane Georges wind field

Hurricane Georges formed near 12.5°N, 41.1°W in the western tropical Atlantic on 17 September, 1998 with a minimum central pressure of 98.7 kPa. It was the fourth hurricane of the 1998 hurricane season. On 19 September, 1998, Hurricane Georges strengthened into the Saffir-Simpson Scale Category 4 with a maximum wind speed of 67.0 m/s. On 26 September, 1998, Hurricane Georges entered the Gulf of Mexico passing through the Straits of Florida. On 27 and 28 September 1998, Hurricane Georges passed through the study area. During this period, Hurricane Georges weakened into a category 2 hurricane with estimated maximum winds of 50 m/s. A track of the hurricane within the study area is shown in Fig.1 as a bold dash-dot line taken from web site http://www.nhc.noaa.gov. The evolution of major parameters of the hurricane is listed in Table 2 (Guiney, 1999).

An extended time series record of vector winds during the passage of Hurricane Georges measured by NOAA Buoy 42040 is shown in Fig. 2. The temporal resolution of the record is 1 h. One can see that northerly winds first and southerly winds later constitute the prevailing components, implying that the eye of the hurricane passed through the buoy from southeast to northwest.

From Fig. 2 we measure that the time interval, for which the negative maximum wind velocity and the positive maximum wind velocity passed over the buoy, is 8 h. From the historical data of the hurricane listed in Table 2, we calculate the translating speed as 3.8 m/s at Sta. C3 and 2.7 m/s at Sta. C1. Assuming a spatially symmetrical hurricane and an overhead passage of the hurricane center through the buoy, we ob-

Table 2. History of 1998 Hurricane Georges in the study area

Date/Time (1998)	Position		Close Sta.	Translation speed/m·s^{-1}	Pressure/kPa	Wind/m·s^{-1}
	north latitude/(°)	west longitude/(°)				
27 Sep./00:00	27.0	86.5			96.9	48.9
06:00	27.6	87.2		4.3	97.0	48.9
12:00	28.2	87.8		4.0	96.2	48.9
18:00	28.8	88.3	C3	3.8	96.2	48.9
28 Sep./00:00	29.3	88.5	NOAA 42040,C1	2.7	96.1	48.9
06:00	29.8	88.7		2.7	96.4	46.3
12:00	30.4	88.9	near shore	3.2	96.5	46.3
18:00	30.6	88.9	land	1.0	98.4	33.5

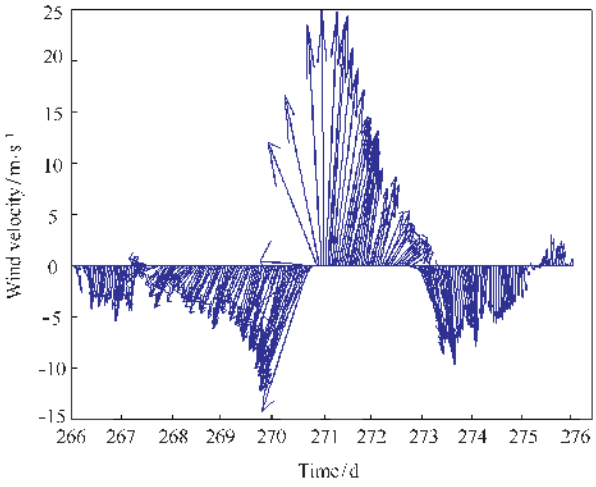

Fig. 2. Sea surface wind vectors measured by NOAA Moored Buoy 42040 during an extended period of the passage of 1998 Hurricane Georges.

tain the radius of maximum wind of the hurricane (Shay and Elsberry, 1987), R_{max}, as 55 km at Sta.C3 and 39 km at Sta.C1, respectively.

We transform the vector winds into the sea surface wind stress using the traditional formula:

$$\tau=\rho_a C_d|U|U,$$

where ρ_a is the air density; U is the sea surface wind speed; and C_d is the drag coefficient in the form of (Garratt, 1977):

$$C_d=(0.75+0.067U_{10})\times10^{-3},$$

where U_{10} is the wind speed measured at 10 m above the sea level. In our case, buoy winds are measured at 5 m above the sea level, i.e., U_5. We convert U_5 using an approximate relation: U_{10}=1.19 U_5, which is derived from an empirical curve measured by Deacon et al. (1956). The calculated wind stress time series give the peak values of the zonal and the meridional components of wind stress are 3.8 and 5.2 N/m^2, respectively.

4 Shallow water response

We use Mooring Station C1 with the water depth of 100 m to demonstrate the response of the shallow water side of continental shelf to the Hurricane Georges. Figure 1 shows that Sta.C1 is on the right hand side of the hurricane track. Meanwhile, from Table 1 we know that the nearest distance to the hurricane center is 114 km, or 2.9 R_{max}. These data and information indicate that Sta.C1 is located within a range with the maximum response or resonance excitation to the hurricane (Chang and Anthes, 1978; Price, 1983).

4.1 Normal mode analysis

The vertical thermal structure at Sta.C1 measured just before the Hurricane Georges came in is shown in Fig. 3. One can see that a top layer is a very thin, warm mixed layer with a depth of about 5 m and water temperature of 30 ℃. Beneath this warm layer, there is a sharp thermocline. The water temperature decreases to 20 ℃ at water depth of 40 m, i. e., a 10 ℃ decrease within 30 m or a vertical temperature gradient of −0.33 ℃/m. Compared with the vertical thermal structure of Sta. C3 shown in Fig. 5, which is 63 km south, we find that the water temperature in the mixed layer at Sta. C1 is only 0.5 ℃ lower than that at Sta. C3, while the water temperature in the thermocline is 5 ℃ lower than that at Sta. C3 at the same depth. This implies that the sharp thermocline at Sta. C1 should be maintained by cold water upwelling.

Using the vertical temperature profile shown in Fig. 3 and a uniform salinity of 35, we calculate an approximate vertical profile of the Brunt–Väisälä fre-

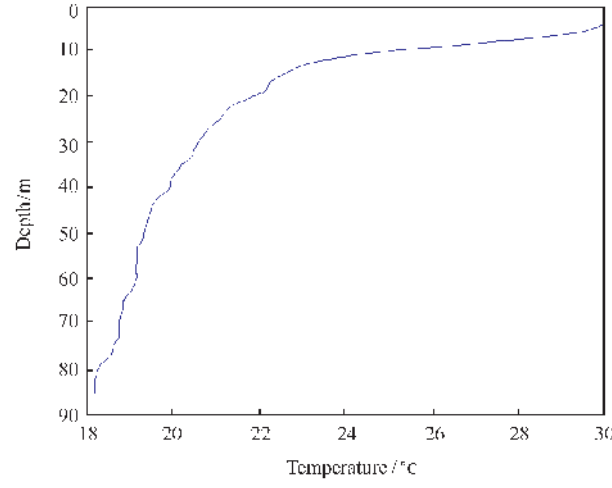

Fig. 3. Vertical thermal structure at Sta. C1.

quencies (N-profile, not shown) (Gill, 1982). We treat this N-profile as an initial condition of ocean stratification at Sta. C1. From this N-profile, we are able to predict the phase speeds, frequencies and time scales of baroclinic modes of inertial oscillation waves using the normal mode solutions derived by Gill (1982, 1984). Here we adopt the physical model of the N-profile developed by Gill in the form of

$$N=\begin{cases}0, & H-H_{\mathrm{mix}}<z<H,\\ s(z_0-Z)^{-1}, & 0<z<H-H_{\mathrm{mix}},\end{cases} \tag{1}$$

where H is the water depth; H_{mix} is the mixed layer depth; z is the vertical axis positive upward; s = 2.8 m/s; and z_0 is a constant to be determined with the observations. The phase speed c_n is given by

$$\left(\frac{s}{c_n}\right)^2=m^2+\frac{1}{4}, \tag{2}$$

where m satisfies

$$\left(n-\frac{1}{2}\right)\pi < m\xi_t < n\pi,$$

in which ξ_t is determined by

$$\xi_t=\ln\left(\frac{z_0}{z_0-(H-H_{\mathrm{mix}})}\right).$$

The frequency for the nth mode inertial wave ω_n is determined by

$$\omega_n^2=f_2+l^2c_n^2, \tag{3}$$

where l (=$2R_{\max}$) is the length scale. The time scale t_n is given by

$$t_n=\frac{\pi}{2(\omega_n-f)}\approx\frac{\pi f}{l^2c_n^2}. \tag{4}$$

In the case of Sta.C1, H = 100 m, H_{mix}=5 m, N (90 m) = 46.4 /ms, f = 71.78 μrad/s, and $2R_{\max}$=78 km. We calculate wave parameters using Eqs(1)~(4). The results are listed in Table 3. The translational speed of the hurricane, U_{h}, as it approached closest to Sta.C1 was 2.7 m/s. Table 3 gives the internal wave phase speed of the first baroclinic mode, c_1, as 1.36 m/s. Thus, the Froude number, U_{h} / c_1, is 2.0 (>1), implying that baroclinic near-inertial waves will be excited in the wake of the hurricane (Geisler, 1970).

Table 3. First five baroclinic normal modes of Sta. C1

Mode (n)	c_n/m·s^{-1}	ω_n/ ×10^{-5}s^{-1}	σ_n(cycles per day)	σ_n/f*	t_n/d	λ_n/km	Rossby / km
1	1.36	7.388	1.017	1.030	8.7	116	19
2	0.56	7.214	0.993	1.006	50.5	49	7.8
3	0.35	7.192	0.990	1.003	130	31	4.9
4	0.25	7.185	0.988	1.001	260	22	3.5
5	0.19	7.182	0.988	1.001	455	17	2.6

∗ f is 0.987 5 cycles per day.

4.2 Ocean current time series analysis

Ocean current velocity profile time series measured at Sta. C1 during the extended 1998 hurricane season from 12 August (day 224) to 8 December (day 342) 1998 are shown in Figs 4a and b. The temporal resolution of the records is 30 min. Ripples along the curves include signals of near-inertial oscillations with the period of about 1 d. One can see that the near-inertial oscillations always existed, though sometimes they strengthened and sometimes weakened. From the records, we estimate that the average peak-to-peak amplitude is on the order of 30 cm/s. The records also show two obvious oscillation strengthening processes, happened at the beginning and the end of September 1998 (around year-days 245 and 270). Those two periods were corresponding to the passages of Hurricane Earl and Hurricane Georges, respectively. During those periods, the oscillation amplitudes obviously increased, implying that the ocean near-inertial oscillation gained huge momentum from hurricanes through air–sea coupling. In particular, during the second event, the amplitudes in the upper surface layer increased almost one order.

4.3 Time–depth–energy density image interpretation

In order to show the evolution process and vertical propagation of the ocean current response clearly, we calculate the ocean current energy density from the current velocity components shown in Figs 4a and b. Assuming a cosine oscillation function, the average

kinematic energy density over a period is

$$\overline{E}_{\mathrm{k}}=\frac{1}{4}\rho A^{2}, \tag{5}$$

where ρ is the water density; and A is the velocity amplitude of a fluid parcel. For discrete data, Eq. (5) has an approximate form

$$\overline{E}_{\mathrm{k}}=\frac{\rho}{4}\left[\frac{\sum_{m=-l}^{l}(u^{2},v^{2})_{i+m}}{2l+1}\right], \tag{6}$$

where u and v are zonal and meridional components of the ocean current velocity, respectively; $i + m$ (= 0, 1, 2,⋯) is a time series number of a data point; $2l + 1$ is a number of data points over the oscillation period, 1 d in our case, implying that l equals to 24.

A time–depth–energy density image from year-days 266 to 276 corresponding to an extended period of the passage of Hurricane Georges is shown in Fig. 4c. One can see that a remarkable feature of the image is that there are two energy peaks. The major one with a peak value of 730 J/m^3 is located above 16 m, and the secondary one with a peak value of 550 J/m^3 is centered at 52 m within a range from 36 to 72 m. Comparing with the vertical thermal structure shown in Fig. 3, we find that the depths of the two peaks are closely associated with the vertical thermal structure. The major peak extends to 16 m, which is about 10 m deeper than the initial mixed layer depth. This increase in the mixed layer

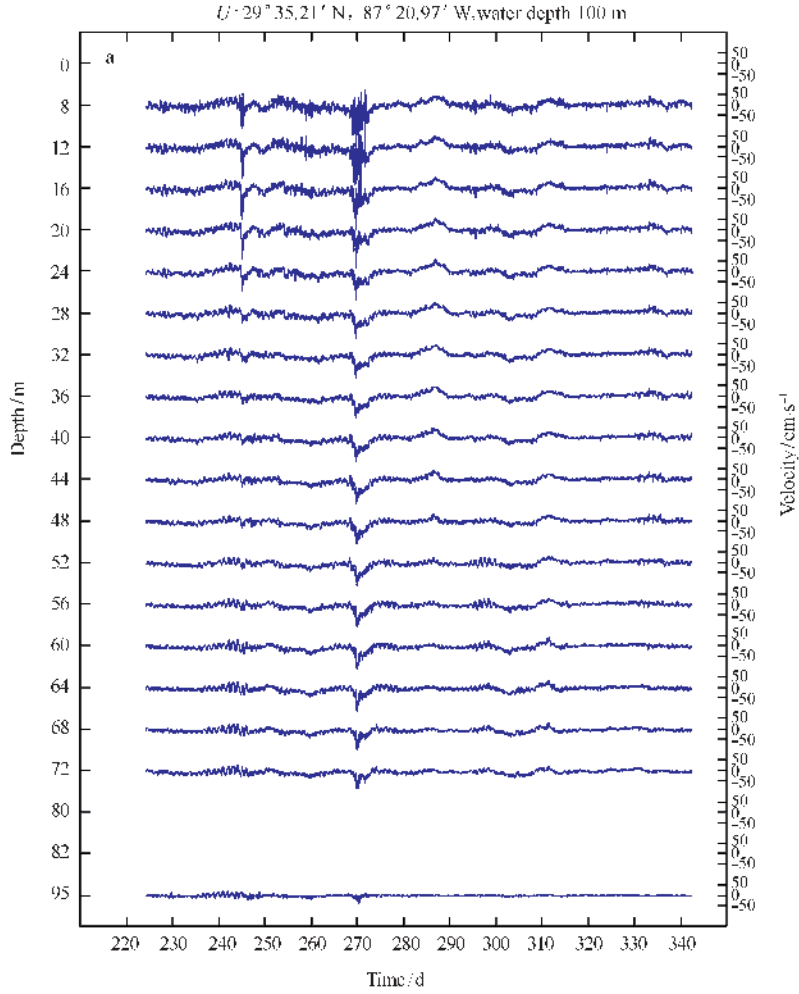

Fig. 4a.

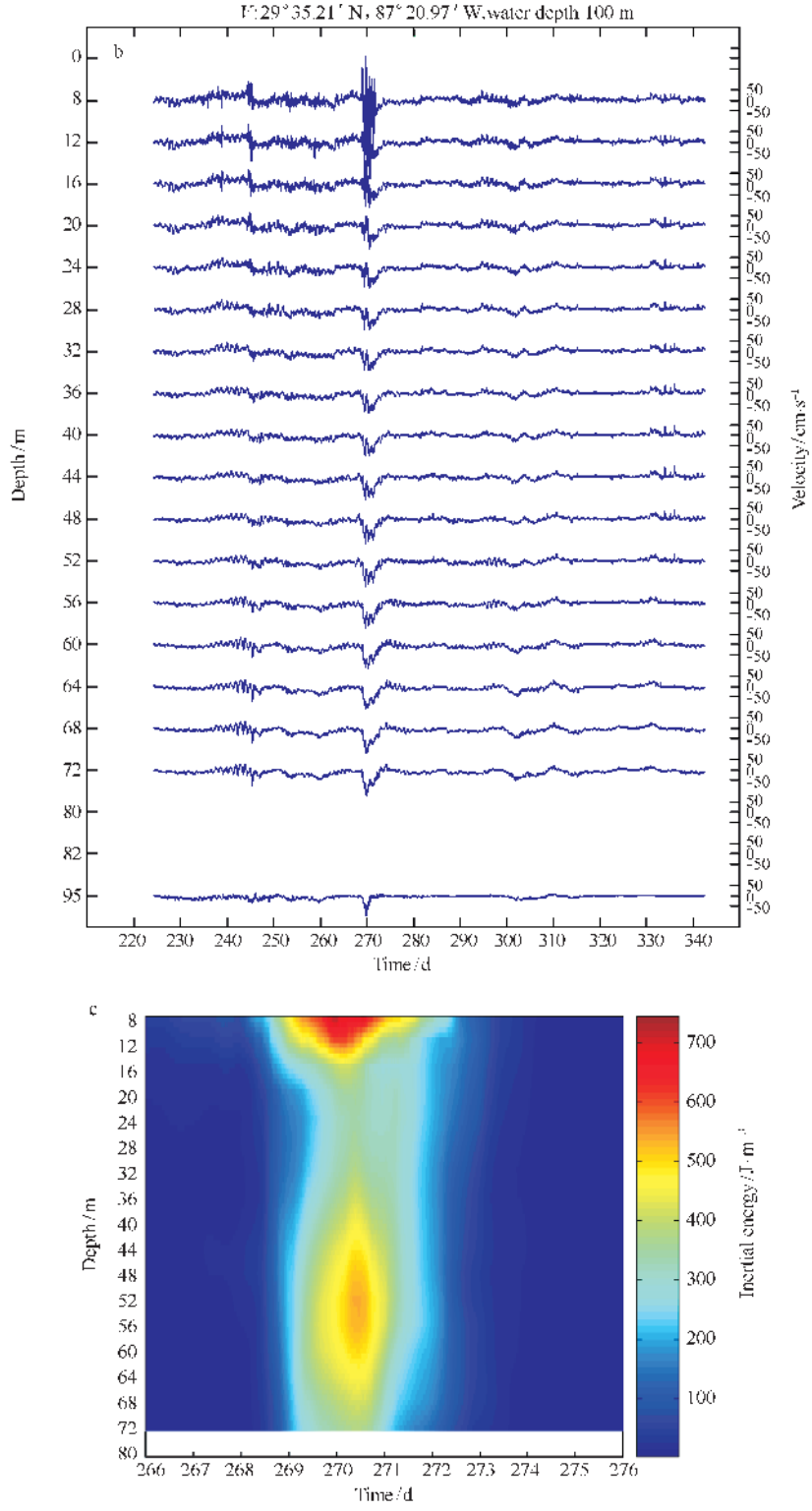

Fig. 4. Field data measured at Sta.C1 during the 1998 hurricane season. Time series data of ocean current components, u (a) and v (b) and time–depth image of near-inertial oscillation energy density (c) calculated with data of a and b from days 266 to 276, 1998 corresponding to the period of the passage of 1998 Hurricane Georges through the study area.

depth may be attributed to the hurricane forcing (Chang, 1985). The secondary peak at 52 m is located in the lower layer of the thermocline. In between the two there is a transitional layer from 16 to 36 m corresponding to the thermocline with high vertical temperature gradient. This evidences that the energy of ocean response propagates downward from the mixed layer to the lower layers through the thermocline. It is of interest to examine the evolution processes of the two peaks. The mixed layer peak formed on year-days 269 (26 September 1998), and reached its maximum intensity and maximum depth on year-days 270. After that the depth of the peak gradually became shallower and finally disappeared on year-days 272. The whole process lasted for about 2.5 d. This time interval coincides with the duration of episodically high wind event. The secondary peak formed and reached its maximum intensity and maximum depth half a day later than the major peak, but disappeared 1 d earlier than the major one. The maximum value of ocean current energy density of the thermocline peak is 75% of the one in the mixed layer. All these facts further indicate that the energy of thermocline peak is radiated from the mixed layer peak. The energy downward propagation rate measured from Fig. 4c is 0.10 cm/s, which is comparable to 0.07 cm/s estimated by Brooks (1983), 0.12 cm/s estimated by Price (1983), 0.08 cm/s simulated by Shay et al. (1990) for the passage of Hurricane Frederic over the same area, and 0.12 cm/s in the case of Tropical Cyclone Ofa [see Fig. 4 in Firing et al. (1997)].

5 Deep water response

We use Sta.C3 with the water depth of 1 300 m to represent the deep water side of continental shelf to the Hurricane Georges. Figure 1 shows that Sta. C3 is also on the right hand side of the hurricane track. Meanwhile, from Table 1 we know that the nearest distance to the hurricane center is 93 km, or $1.7R_{max}$, implying that Sta.C3 is also located within a range with the maximum response or resonance excitation to the hurricane.

5.1 Normal mode analysis

The vertical thermal structure of Sta. C3 measured just before the Hurricane Georges came in is shown in Fig. 5. One can see that there is a warm mixed layer with a depth of about 30 m and water temperature of 30.5 ℃ on the top of thermocline. The water temperature decreases to 21 ℃ at depth of 100 m, i.e., a 9.5 ℃ decrease within 70 m or a vertical temperature gradient of –0.14 ℃/m, which is not strong as the case at Sta.C1, implying that Sta. C3 was beyond the seasonally coastal upwelling area.

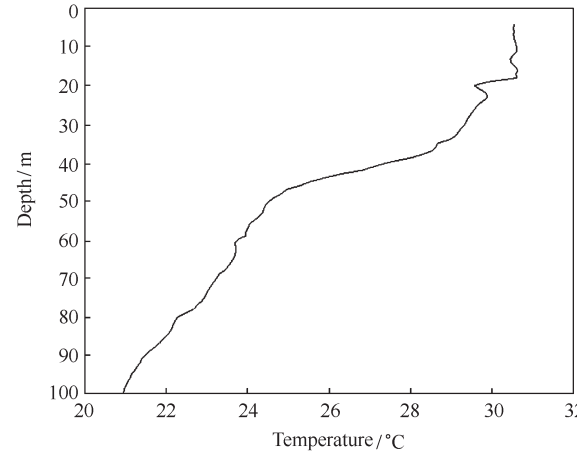

Fig. 5. Same as Fig. 3 but for Sta. C3.

Using the same method as Sta. C1 we calculate the phase speeds, frequencies and time scales of baroclinic modes of inertial oscillation waves. The results are listed in Table 4. One can see that the internal wave phase speed of the first baroclinic mode, c_1, is 2.50 m/s. The translational speed of the hurricane, U_h, as it approached closest to Sta.C3 was 3.8 m/s. Thus, the Froude number is 1.5, implying that baroclinic near-inertial waves will be excited in the wake of the hurricane.

5.2 Ocean current response analysis

Ocean current velocity profile time series mea-

Table 4. First five baroclinic normal modes of Sta. C3

Mode (n)	c_n/m·s^{-1}	ω_n / ×10^{-5}s^{-1}	σ_n(cycles per day)	σ_n/f*	t_n/d	λ_n/km	Rossby / km
1	2.50	7.405	1.019	1.051	25.1	212	35
2	1.36	7.155	0.984	1.015	17	119	19
3	0.79	7.084	0.975	1.005	51	70	11
4	0.62	7.070	0.973	1.003	83	55	8.8
5	0.51	7.063	0.972	1.002	121	45	7.2

* f is 0.969 7 cycles per day.

sured at Sta. C3 from 12 August to 8 December 1998 are shown in Figs 6a and b. As mentioned above, we use this station to represent the deep water side of the shelf-break. The temporal resolution of the records also is 30 min. One can see that the near-inertial oscillations with the average period of about 1 d always existed during the season and in the whole water column. The data sets also show two obvious strengthening processes of inertial oscillations happened at the beginning and the end of September 1998, corresponding to the passages of Hurricane Earl and Hurricane Georges, respectively. Comparing with Figs 4a and b, we find that amplitudes of strengthened oscillation during the two events are larger than those in the shallow water side and the response time is longer. This implies that the deep water side of the shelf-break has gained more energy from the hurricane, because the hurricane passed through the deep water side first and the shallow water side later. During the passage the intensity of hurricane gradually weakened.

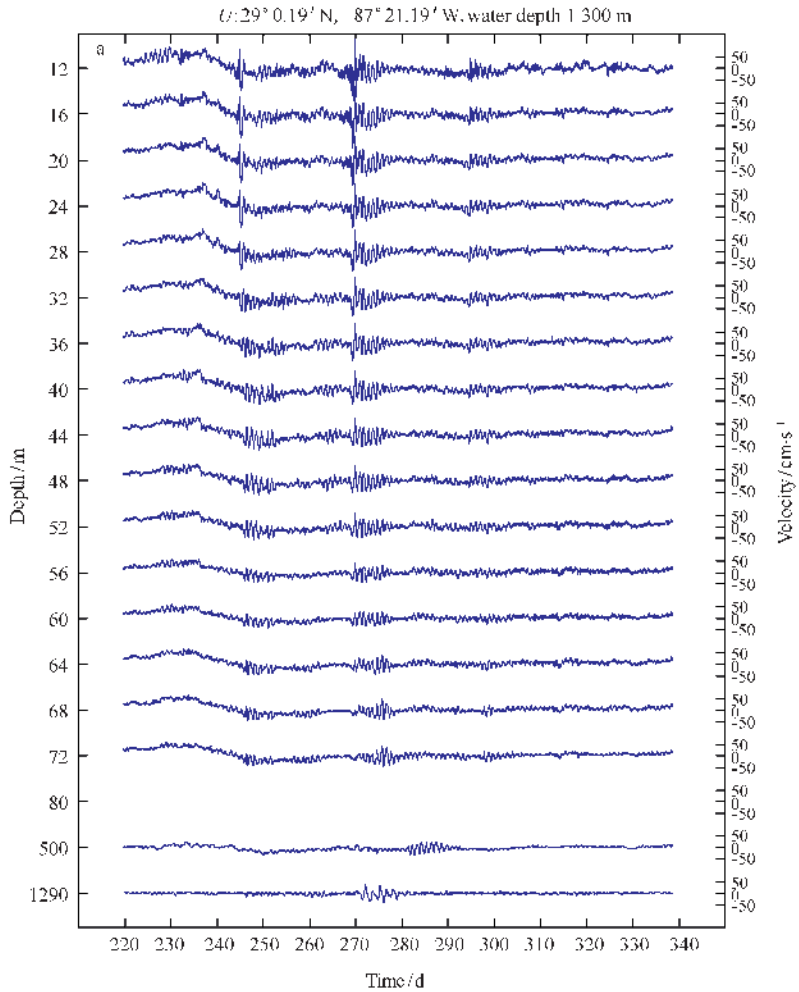

Fig. 6a.

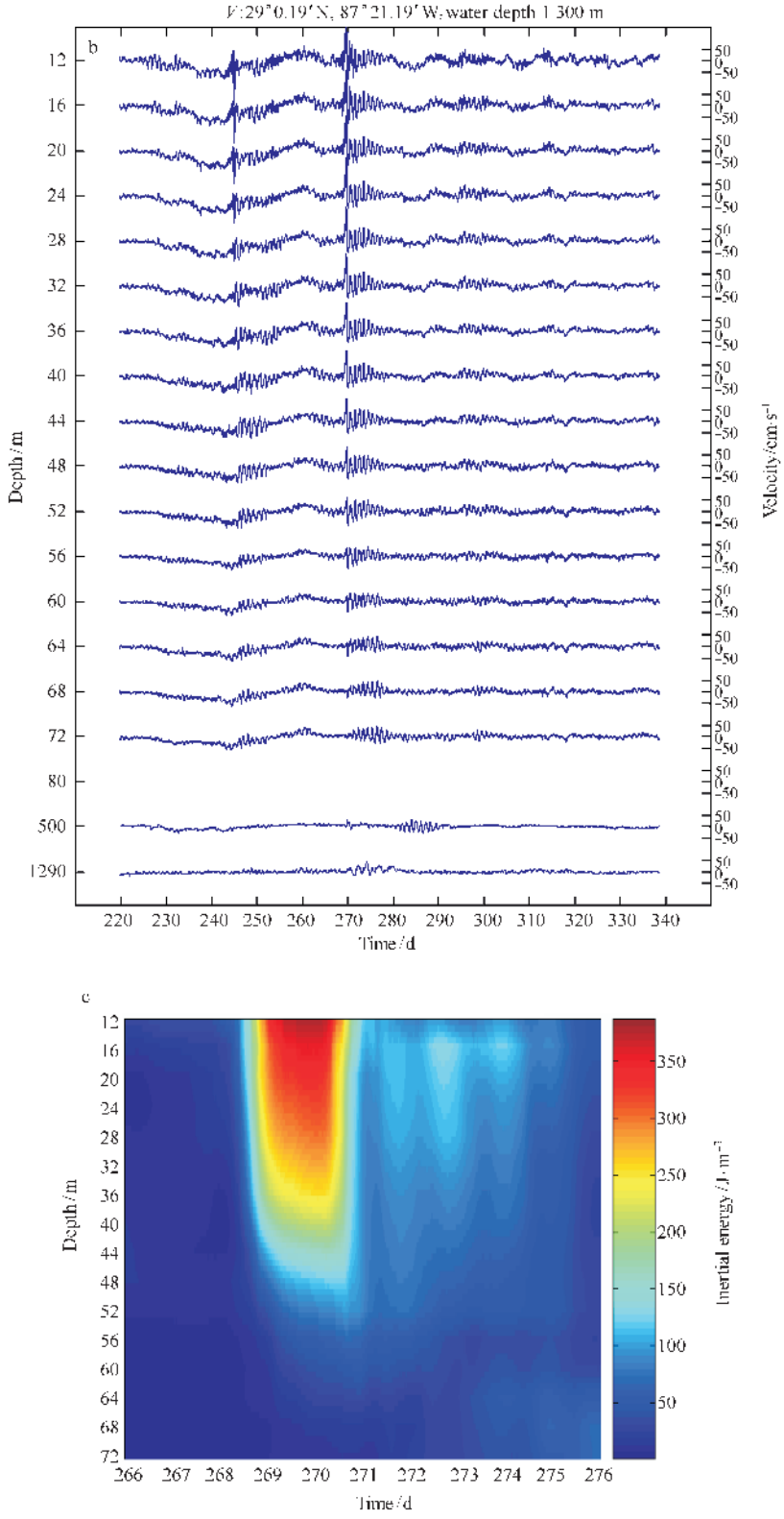

Fig. 6. Same as Fig. 4 but for Sta. C3.

The time–depth–energy density image from days 266 to 276 corresponding to the extended period of the passage of Hurricane Georges is shown in Fig. 6c. One can see that the image shows only one peak located above 72 m, of which a maximum value is 380 J/m^3 located at the surface layer above 16 m. The lower border of the peak reaches 50 m, if the energy density of 100 J/m^3 is chosen as a boundary between the peak and surrounding waters. Comparing with the vertical thermal structure in Fig. 5, we find that this depth is the local mixed layer depth. The peak formed in the upper surface layer on day 269, and reached its maximum intensity and maximum depth on day 270. After that the depth of the peak became shallower quickly on day 271. This major peak lasted for 2 d. Following this major peak, three minor peaks with the energy density higher than 100 J/m^3 were consequential in the following 5 d. According to Geisler (1970) and Gill (1984), these minor peaks should be signatures of baroclinic inertial waves in the wake of the hurricane. There is not the secondary peak or the beam being observed, because below 72 m there are only two data sets measured at 500 and 1 290 m available. However, examining the curves measured at 500 m shown in Figs 6a and b, one can see that a near-inertial wave packet still existed between days 280 and 290.

5.3 Vertical dispersion

From ocean current velocity profile time series shown in Figs 6a and b, we may extract the information on the vertical dispersion of near-initial waves during the passage of 1998 Hurricane Georges. Examining the evolution of the waves during their propagating vertically, one can see that the near-inertial wave packet generated in the mixed layer in fact consists of two modes, P1 and P2. Mode P1 led by the first wave was generated on day 270 (27 September 1998), and characterized by fast vertical decay. Mode P2 represented by the sixth wave was generated on day 274 (1 October 1998), and characterized by slow vertical decay. Figure 7 shows their vertical decay processes. One can see that the velocity amplitude of Mode P1 (Series 1) decays 92% from a maximum value of 126.3 cm/s at 12 m to 10 cm/s at 72 m. On the other hand, the velocity amplitude of Mode P2 (Series 2) decays 40% from a maximum value of 64.9 cm/s at 20 m to 38.9 cm/s at 60 m. From 60 to 72 m, the amplitude changes little. Even at 500 m, Mode P2 existed till day 290 (17 October 1998). The maximum velocity amplitude still reaches 38.9 cm/s, which is 66% of that at 72 m. The downward propagation rate of Mode P2 is estimated as 0.05 cm/s, which is comparable to 0.10 cm/s in the case of Sta. C1.

The evolution processes of modes P1 and P2 show the following distinctions. (1) From Fig. 7, we calculate that the decay rate of velocity amplitude in P1 is 0.020 s^{-1}, and in the mixed layer the decay rate of P2 is 0.006 9 s^{-1}. In other words, the decay rate of P1 is as large as 2.9 times that of P2. (2) In the thermocline and deep layer below 60 m, P1 decays quickly to null at 78 m, implying that P1 is basically trapped in the mixed layer. In contrast, P2 is capable of penetrating the mixed layer into deep layers. (3) In the time domain, P1 was generated first when the hurricane was close to the station, and existed only for few early days of the event. On the other hand, the data measured at the thermocline and deep layer (see curves of 72 and 500 m in Figs 6a and b) indicate that the earliest day on that P2 could be identified was day 271 (September 28), the third day of the event. At that day the center of Hurricane Georges had left over the station (see Fig.1), implying that P2 existed in the wake of the hurricane. There seems to be an overlap between P1 and P2.

The distinctive behavior of P1 and P2 indicates their different dynamic natures. In fact, we have interpreted P2 as a baroclinic near-inertial wave mode in the above section. Similarity of its vertical profile of velocity amplitude shown in Fig. 7 to that of baroclinic mode 1 further enhances this interpretation. For P1, owing to its quick response rate and fast decay rate, which are the typical features of barotropic pressure waves (Chang, 1985), it is reasonable to interpret it as a

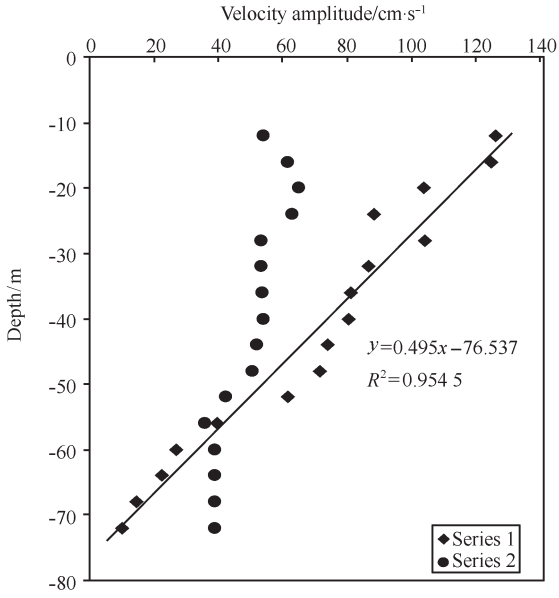

Fig. 7. Vertical dispersion of two sub-packets of near-inertial waves at Sta. C3.

barotropic near-inertial wave mode.

6 Blue shift of near-inertial response frequency

Previous investigations indicate that the frequency of hurricane-induced near-inertial oscillation would shift above the local inertial frequency, called "the blue shift" (Price, 1983; Gill, 1984; Shay and Elsberry, 1987; Shay et al., 1990). Normal mode diagnosis in this study gives the blue shifts in the frequencies from 1.001 *f* to 1.030 *f* for Sta. C1 and from 1.002*f* to 1.051*f* for Sta. C3 as listed in Tables 3 and 4. Of course, the real case should be derived from field observations. In order to do so, in situ measurements of the currents need to be pre-processed, because the data contain signals generated by various ocean processes. These processes obviously include the high frequency ocean surface waves that can penetrate to a certain depth and low frequency variations induced possibly by eddy intrusion and topography Rossby waves. The other important issue in our case is that the ocean response to the hurricane passage is an episodic event. Therefore, a data processing method must be found for filtering the near-inertial oscillation signals out and holding the hurricane signals. Tests indicate that the empirical mode Decomposition (EMD) method developed by Huang et al. (1998) gave the best results for processing these non-stationary current data. Using the EMD method, the time series current measurements are decomposed into a group of empirical modes. The modes with frequencies close to the inertial oscillation frequency are chosen for rebuilding new data sets. These band-pass-filtered data sets are least-squares fitted to an empirical function

$$u=-a[\operatorname{sech}^2(t)+G(t)\mathrm{e}^{-\mathrm{i}\sigma t}]+b\mathrm{e}^{-\mathrm{i}(\sigma t-\theta)}, \qquad (7)$$

where a, b, $G(t)$, σ, and θ are adjustable. Then, the frequency of near-inertial oscillation, σ, can be determined. The results derived from the current measurements from days 265 to 277, 1998 at depths of 8 and 52 m at Sta. C1 as well as 12 and 52 m at Sta. C3 are listed in Table 5. One can see that all frequencies shift above the local inertial frequency. At Sta.C1, in the mixed layer represented by the case of depth 8 m, the average frequency is 1.04*f*, close to the diagnosed frequency of the first baroclinic mode, 1.030*f*, and in the thermocline represented by the case of depth 52 m, the average frequency increases to 1.07*f* as predicted by Price (1983) and Kundu and Thomson (1985). At Sta. C3, all frequencies are a little smaller than the di-

Table 5. Frequencies of near-inertial oscillations determined by an empirical function method

Station	Depth/m	Velocity component	γ*	σ(cycles per day)	σ/f**/h	Period/h
C1	8	*u*	0.40	1.02	1.03	23.5
	8	*v*	0.43	1.04	1.05	23.1
	52	*u*	0.53	1.08	1.09	22.2
	52	*v*	0.79	1.04	1.05	23.1
C3	12	*u*	0.69	1.00	1.03	24.0
	12	*v*	0.69	1.01	1.04	23.8
	52	*u*	0.83	0.99	1.02	24.2
	52	*v*	0.85	0.99	1.02	24.2

* Correlation coefficient between the empirical function and observations.

** *f* is 0.987 5 cycles per day at Sta. C1, and 0.969 7 cycles per day at Sta. C3.

agnosed frequency of the first mode, 1.051*f*. The average frequency decreases from 1.035*f* in the mixed layer represented by the case of depth of 12 m to 1.02*f* in the thermocline represented by 52 m, implying a trend for the shift in the oscillation frequency towards *f* with the depth. This agrees with observations in the same region by Gaul (1967).

A correlation coefficient of each case is appended in the table. One can see that except two surface layer cases of Sta. C1, the average correlation coefficient of other six cases is 0.73, indicating that in general the empirical function fits the measured currents quite well. In the cases of 8 m at Sta. C1, the correlation coefficients are relatively low, implying that the ocean response seems to be more complicated in the case of surface layer of the shallow water.

7 Conclusions and discussion

This study indicates that the shelf-break ocean, no matter its shallow water side or deep water side, has an almost immediate response to passage of a hurricane. The oscillation peak-to-peak amplitudes in the surface layers during the passage of 1998 Hurricane Georges strengthen to the order of 100 cm/s.

Time–depth near-inertial oscillation energy density images show that on the shallow water side, a major peak forms in the mixed layer and a secondary peak is observed in the lower layer. The response disappears quickly after the hurricane moves out the area. On the deep water side, only one peak is observed in the mixed layer. There is the consequential response observed, which is in the form of a wave-like tail of the major peak, and lasts for 5 d after the hurricane moves out the area. We believe that this wave-like tail represents the ocean internal wave generated in the wakes of the hurricane.

Long-term and high resolution current measurements provide a unique chance for vertical dispersion analysis of the hurricane-induced near-inertial oscillations. The results reveal that the near-initial wave mode in the deep water consists of two subpackets. One is a barotropic wave mode characterized by features of barotropic pressure waves. The vertical decay rate of velocity amplitude reaches as fast as 0.020 s^{-1}. The other is baroclinic wave packet characterized by a slow decay rate of 0.006 9 s^{-1}.

The band-pass-filtering method developed based on the empirical mode decomposition is used to determine the near-inertial wave frequency. The results indicate that all frequencies shift above the local inertial frequency on and off the shelf. On the shelf, the average frequency is 1.04*f* in the mixed layer, close to the diagnosed frequency of the first baroclinic mode, and the average frequency increases to 1.07*f* in the thermocline. Off the shelf, all frequencies are a little smaller than the diagnosed frequency of the first mode. The average frequency decreases from 1.035*f* in the mixed layer to 1.02*f* in the thermocline, implying a trend for the shift in the oscillation frequency towards *f* with the depth.

The tides are a factor to mix with current observations and to have possible influences on our data analysis, because the periods of the near-inertial oscillations are very close to those of the diurnal tides. We use the scale analysis for estimation of the influences. The near-inertial oscillations and tides have different features of vertical damping because of different generation forces. The near-inertial oscillations are generated by the wind stress on the ocean surface, therefore, they damp down quickly from the surface layer to the deep layer. On the other hand, the tides are motion of the whole water body, they may damp down only because of bottom friction. Therefore, in the current measurements at the deep water, the tidal currents should become dominant components, if the near-inertial oscillations are not extremely strong. Examining the ocean current time series data beyond the hurricane periods shown in Figs 4a and b and 6a and b, at 72 m for Sta.C1 and at 500 m for Sta.C3 after day 320, we find that the current velocity never exceeded 5 cm/s. This value may serve as an estimate of the maxi-

mum tidal currents. On the other hand, the ocean current velocity amplitudes always exceeded 100 cm/s during the passage of Hurricane Georges. Therefore, we believe that the tidal influences are not important for the special case analysis of the ocean response to the extremely high wind event.

Acknowledgements

Preliminary analysis was done when Zheng Quanan and Pan Jiayi worked at University of Delaware. The authors express their thanks to Yuan Ying and Zhao Zhongxiang for help in data processing. This work was supported by the NASA of USA under contract No.E99−NAG5−5149.

References

Brooks D. 1983. The wake of hurricane Allen in the western Gulf of Mexico. Journal of Physical Oceanography, 13: 117~129

Chang S W. 1985. Deep ocean response to hurricanes as revealed by an ocean model with free surface: Part I. Axisymmetric case. Journal of Physical Oceanography, 15: 1 847~1 858

Chang S W, Anthes R A. 1978. Numerical simulations of the ocean's nonlinear baroclinic response to translating hurricanes. Journal of Physical Oceanography, 8: 468~480

Deacon E L, Sheppard P A, Webb E K. 1956. Wind profiles over the sea and the drag at the sea surface. Australian Journal of Physics, 9: 511~514

Firing E, Lien R-C, Muller P. 1997. Observations of strong inertial oscillations after the passage of Tropical Cyclone Ofa. Journal of Geophysical Research, 102: 3 317~3 322

Garratt J R. 1977. Review of drag coefficients over oceans and continents. Monthly Weather Review, 105: 915~929

Gaul R D. 1967. Circulation over the Continental Margin of the Northeast Gulf of Mexico, Rep, n 286−d. Texas A&M University, 36

Geisler J E. 1970. Linear theory on the response of a two-layer ocean to moving hurricane. Geophysical Fluid Dynamics, 1: 249~272

Gill A E. 1982. Atmosphere−Ocean Dynamics. New York: Academic Press, 662

Gill A E. 1984. On the behavior of internal waves in the wake of storms. Journal of Physical Oceanography, 14: 1 129~1 151

Gold E. 1908. Barometric Gradient and Wind Force. Meteorol Offi, M O 190, HM Stationery Office, London

Greatbatch R J. 1983. On the response of the ocean to a moving storm: the nonlinear dynamics. Journal of Physical Oceanography, 13: 357~367

Greatbatch R J. 1984. On the response of the ocean to a moving storm: parameters and scales. Journal of Physical Oceanography, 14: 59~78

Guiney J L. 1999. Hurricane Georges 15 September—01 October 1998, Preliminary Report. NOAA National Hurricane Center, 5 January 1999, 30

Halpern D. 1974. Observations of the deepening of the wind-mixed layer in the North-East Pacific Ocean. Journal of Physical Oceanography, 4: 454~466

Huang N E, Shen Z, Long S R, et al. 1998. The empirical mode decomposition and the Hilbert spectrum for nonlinear and non-stationary time series analysis. Proceedings of the Royal Society of London A, 454: 903~995

Keen T R, Allen S E. 2000. The generation of internal waves on the continental shelf by Hurricane Andrew. Journal of Geophysical Research, 105: 26 203~26 224

Kundu P K. 1976. An analysis of inertial oscillations observed near Oregon coast. Journal of Physical Oceanography, 6: 879~893

Kundu P K, Thomson R E. 1985. Inertial oscillations due to a moving front. Journal of Physical Oceanography, 15: 1 076~1 084

Minerals Management Service. 1999. DeSoto Canyon Eddy Intrusion Study Annual Report: Year 3. MMS, Pub No. 99~56

Pollard R T. 1970. On the generation by winds of inertial waves in the ocean. Deep-Sea Research, 17: 795~812

Price J F. 1981. Upper ocean response to a hurricane. Journal of Physical Oceanography, 11: 153~175

Price J F. 1983. Internal wave wake of a moving storm: Part I. Scales, energy budget and observations. Journal of Physical Oceanography, 13: 949~965

Shay L K, Black P G, Mariano A J, et al. 1992. Upper ocean response to Hurricane Gilbert. Journal of Geophysical Research, 97: 20 227~20 248

Shay L K, Chang S W, Elsberry R L. 1990. Free surface effects on the near-inertial ocean current response to a hurricane. Journal of Physical Oceanography, 20: 1 405~1 424

Shay L K, Elsberry R L. 1987. Near-inertial ocean current response to Hurricane Frederic. Journal of Physical Oceanography, 17: 1 249~1 269